THEORETICAL & APPLIED MECHANICS LETTERS **2**, 052003 (2012)

Magnetohydrodynamics convective flow in a vertical slot through a porous medium

Rajnish Kumar,[1, a)] and Bal G. Prasad[2]
[1)] *Department of Applied Mathematics, Birla Institute of Technology, Patna Campus, Mesra Bihar, India*
[2)] *Department of Mathematics, B.N. College, Patna University, Bihar, India*

(Received 9 May 2012; accepted 18 July 2012; published online 10 September 2012)

Abstract An analysis is presented with magnetohydrodynamics natural convective flow of a viscous Newtonian fluid saturated porous medium in a vertical slot. The flow in the porous media has been modeled using the Brinkman model. The fully-developed two-dimensional flow from capped to open ends is considered for which a continuum of solutions is obtained. The influence of pertinent parameters on the flow is delineated and appropriate conclusions are drawn. The asymptotic behaviour and the volume flux are analyzed and incorporated graphically for the three-parameter family of solution.
 [doi:10.1063/2.1205203]

Keywords natural convection, porous medium, magnetohydrodynamics, Brinkman model, vertical slot

The requirements of modern technology have simulated the interest in fluid flow studies, which involves the interaction of several phenomena. One such study is the natural convection of magnetohydrodynamics (MHD) flow in porous medium which not only possesses a theoretical appeal but also models many biological and engineering applications such as MHD generators and accelerators in geophysics, plasma studies, biomagneto fluids, in design of underground water energy storage system, soil-sciences, astrophysics, nuclear power reactors and so on. Recent papers by Weidman and Medina,[1] Turkyilmazoglu[2,3] et al. show considerable research activities involving such types of flow.

The earliest studies of the convection regime with application to open cavities can be traced back to Prandtl[4] who investigated the flow along an inclined surface where there is an excess of temperature over that of the stratified ambient fluid. In a very significant study, Bühler[5] dealt with the problem of natural convection of a clear fluid in the conduction regime and investigated the range of existence for flows with and without back flow. Weidman[6] extended his work in the convection regime to encompass Newtonian flow of a clear fluid. Magyari[7] proposed a new method of solution which depends on the reduction of the problem to its normal modes by applying a complex matrix similarity transformation, and some new invariant relationships involving the heat flux and the shear stress in the flow were also discussed. Further, this problem has been extended to the porous medium case by Weidman and Medina.[1] It was shown that the Brinkman model, valid for sufficiently large porosity and governed by parameter α, allows one to connect Bühler's conduction regime flow at low α to a near-Darcy convection regime boundary layer flow at high α.

In the present treatise the mathematical analysis of Weidman and Medina[1] is extended to include the magnetic parameter in Cartesian axisymmetric framework coupled with the effect of cross-channel variation of the reference temperature. A literature survey reveals that no published accounts are available regarding the present concern. Efforts are focused on identifying the influence of non-dimensional parameters, such as porosity and magnetic parameter. In the following, the problem is formulated, analyzed, solved and discussed.

Natural convective flow of a viscous conducting fluid saturated porous medium between vertical rigid walls in a uniform gravitational field g is considered under the influence of uniform transverse magnetic field. The fluid has viscosity μ, thermal expansion coefficient γ, and $\tilde{\mu}$ is the effective viscosity of the fluid saturated porous matrix. A magnetic field of uniform strength B_0 is applied in the direction of normal to the flow and the induced magnetic field is neglected.

We make use of a Cartesian coordinate system centered in the gap with x^* directed upwards antiparallel to gravity and y^* the cross-channel coordinate, with respective velocity components (u^*, v^*). The porous end caps shown in Fig. 1 are for illustration purposes only. We do not model the pressure drop across the end caps and only consider the fully-developed flow far from the end caps. The thermal boundary conditions on the vertical walls are noted in Fig. 1 and the velocity conditions are those of impermeability and no-slip.

Following Bühler,[5] an important point concerning the problem is that the position of the reference temperature T_0 for calculating the density ρ using the Boussinesq approximation

$$\rho = \rho_0 \left[1 - \gamma \left(T - T_0\right)\right] \tag{1}$$

moves continuously from the centre of the gap for a channel with capped end to the cold wall for an open-ended channel. There is no loss of generality if we take the right wall to be hot relative to the left wall so that $\Delta T = (T_2 - T_1) > 0$.

Away from the top and bottom ends of the cavity, the flow is rectilinear so that $u^* = u^*(y)$, $v^* = 0$ in

[a)] Corresponding author. Email: rajnish.bitpatna@gmail.com.

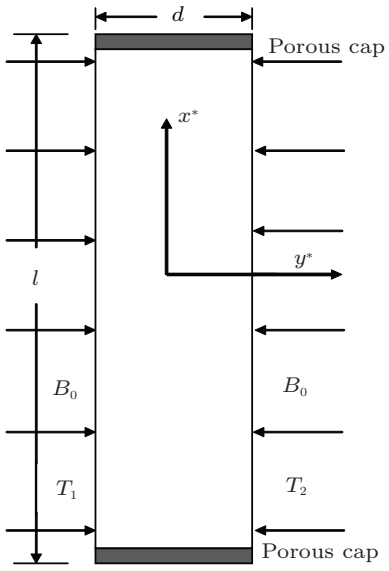

Fig. 1. Schematic drawing of the porous slab of height l showing the porous end caps and the dimensional coordinate system.

which case the continuity equation $\partial u^*/\partial x + \partial v^*/\partial x = 0$ is satisfied identically. Assuming no imposed external pressure gradient, the momentum and energy equations governing the flow may be written as

$$\frac{\mu}{K}u^* = -\frac{\partial p}{\partial x^*} + \tilde{\mu}\frac{\partial^2 u^*}{\partial y^{*2}} - \rho g - \sigma B_0^2 u^*, \tag{2}$$

$$\frac{\partial^2 T}{\partial y^{*2}} = 0. \tag{3}$$

Using the Boussinesq approximation (1), the Brinkmann Eq. (2) yields

$$\begin{aligned}\frac{\mu}{K}u^* &= -\frac{\partial p}{\partial x^*} + \tilde{\mu}\frac{\partial^2 u^*}{\partial y^{*2}} - \rho_0 g + \\ &\rho_0 g\gamma\left(T - T_0\right) - \sigma B_0^2 u^* = \\ &-\frac{\partial}{\partial x^*}\left(p + \rho_0 g x^*\right) + \tilde{\mu}\frac{\partial^2 u^*}{\partial y^{*2}} + \\ &\rho_0 g\gamma\left(T - T_0\right) - \sigma B_0^2 u^*.\end{aligned} \tag{4}$$

In the asymptotic state of fully developed free convection flow in a long vertical channel, the gradient of the pressure excess $(p + \rho_0 g x^*)$ above the hydrostatic pressure $(-\rho_0 g x^*)$ goes to zero and Eq. (4) becomes

$$\tilde{\mu}\frac{\partial^2 u^*}{\partial y^{*2}} = \frac{\mu}{K}u^* + \sigma B_0^2 u^* - \rho_0 g\gamma\left(T - T_0\right). \tag{5}$$

In order to transform the above system of partial differential equations into a non-dimensionless form, use will be made of the following transformations

$$y^* = \frac{y}{d},\ u^* = \frac{\rho_0 g\gamma K\Delta T\, u}{\mu},\ M = \frac{\sigma B_0^2 d^2}{\mu},$$

$$Da = \frac{K}{d^2},\ \theta = \frac{T - T_0}{\Delta T}.$$

Using above dimensionless quantities, we obtain the dimensionless governing equations as

$$\frac{\partial^2 u}{\partial y^2} - \left(\alpha^2 + M^2\right)u = -\alpha^2\theta, \tag{6}$$

$$\frac{\partial^2 \theta}{\partial y^2} = 0. \tag{7}$$

The governing parameters are M (the Hartmann number) and $\alpha^2 = (1/N)Da$, where $N = \tilde{\mu}/\mu$ is the viscosity ratio and Da is the Darcy number.

The no-slip velocity conditions and the isothermal wall conditions are, respectively

$$\begin{aligned}&u\left(-1/2\right) = 0, \quad u\left(1/2\right) = 0, \\ &\theta\left(-1/2\right) = -\theta_0, \quad \theta(1/2) = 1 - \theta_0,\end{aligned} \tag{8}$$

wherein the parameter θ_0 measures the continuous cross-channel variation of the reference temperature T_0 used to calculate the density in Eq. (1), namely

$$T_0 = T_1 + \theta_0\Delta T. \tag{9}$$

The temperature field satisfying the temperature boundary conditions (8) can be obtained as

$$\theta\left(y\right) = y + \left(\frac{1}{2} - \theta_0\right). \tag{10}$$

Inserting Eq. (10) into Eq. (6) gives the inhomogeneous ordinary differential equation for the velocity field, the general solution of which is readily determined to be

$$\begin{aligned}u\left(y\right) = {} & C_1\cosh(\sqrt{\alpha^2 + M^2}y) + \\ & C_2\sinh(\sqrt{\alpha^2 + M^2}y) + \\ & \frac{\alpha^2}{\alpha^2 + M^2}\left[y + \left(\frac{1}{2} - \theta_0\right)\right].\end{aligned} \tag{11}$$

Application of the velocity boundary conditions in Eq. (6) gives the desired solution

$$\begin{aligned}u\left(y\right) = {} & \frac{\alpha^2}{\alpha^2 + M^2}\left\{y + \left(\frac{1}{2} - \theta_0\right)\cdot\right. \\ & \left[1 - \frac{\cosh(\sqrt{\alpha^2 + M^2}y)}{\cosh\left(\sqrt{\alpha^2 + M^2}/2\right)}\right] - \\ & \left.\frac{1}{2}\frac{\sinh(\sqrt{\alpha^2 + M^2}y)}{\sinh\left(\sqrt{\alpha^2 + M^2}/2\right)}\right\}.\end{aligned} \tag{12}$$

Hence the above equation represents a three-parameter family of solutions, depending upon α, M and θ_0.

The normalized planar volume flux up the cavity is given by

$$Q = Q^*/\left(\rho_0 g\gamma K d\Delta T/\mu\right).$$

The only contribution comes from the symmetric portion of the velocity profile which, when investigated across the gap, yields

$$Q = \frac{\alpha^2}{\alpha^2 + M^2}\cdot\left(\frac{1}{2} - \theta_0\right).$$

Table 1. Limiting parameter values for capped and open ends.

Condition	Flow rate	Reference temperature	Parameter
Capped end	$Q = 0$	$T_0 = (T_1 + T_2)/2$	$\theta_0 = 1/2$
Open end	$Q = Q_{\max}$	$T_0 = T_1 + \theta_0 \Delta T$	$\theta_0 = 0$

$$\left[1 - \frac{\tanh\left(\sqrt{\alpha^2 + M^2}/2\right)}{\sqrt{\alpha^2 + M^2}/2}\right]. \tag{13}$$

When $\theta_0 = 1/2$, it is evident that the cavity is closed since $Q = 0$. As θ_0 decreases to $\theta_0 = 0$, the porous end caps tend to the porosity of the fluid saturated medium. Maximum through flow occurs at $\theta_0 = 0$ in Eq. (13), which gives

$$Q_{\max} = \frac{\alpha^2}{\alpha^2 + M^2} \cdot \left[1 - \frac{\tanh\left(\sqrt{\alpha^2 + M^2}/2\right)}{\sqrt{\alpha^2 + M^2}/2}\right]. \tag{14}$$

These results are summarized in Table 1.

As θ_0 decreases from its maximum value $\theta_0 = 1/2$, there comes a value $\theta_0 = (\theta_0)_c$ for incipient reverse flow which occurs on the left cold wall. The condition for incipient backflow is thus given by

$$\left.\frac{\mathrm{d}u}{\mathrm{d}y}\right|_{y=-1/2} = 0, \tag{15}$$

which gives rise to the equation for the critical value of θ_0,

$$(\theta_0)_c = \frac{1}{2} + \left[\frac{2 - \sqrt{\alpha^2 + M^2}\coth\left(\sqrt{\alpha^2 + M^2}/2\right)}{2\sqrt{\alpha^2 + M^2}\tanh\left(\sqrt{\alpha^2 + M^2}/2\right)}\right]. \tag{16}$$

It is of practical significance to obtain the asymptotic behaviour of the results when α is very small (in the limit $\alpha \to 0$) corresponding to a clear fluid and when α is very large (in the limit $\alpha \to \infty$) corresponding to Darcy flow. In both the cases the temperature distributions across the gap are the same linear profiles Eq. (10) dependent only on θ_0.

In the limit $\alpha \to 0$ the leading behaviour of the velocity fluid is given by

$$u(y) \sim \frac{1}{M^2}\left\{y + \left(\frac{1}{2} - \theta_0\right)\left[1 - \frac{\cosh My}{\cosh(M/2)}\right] - \frac{1}{2}\frac{\sinh My}{\sinh(M/2)}\right\} \cdot \alpha^2 + O\left(\alpha^4\right). \tag{17}$$

When properly scaled for a clear fluid through a porous medium in the absence of magnetic field, the leading $O\left(\alpha^2\right)$ is seen to reproduce the results of Bühler[5] which in the present notation is given in Weidman[6], Weidman and Medina.[1]

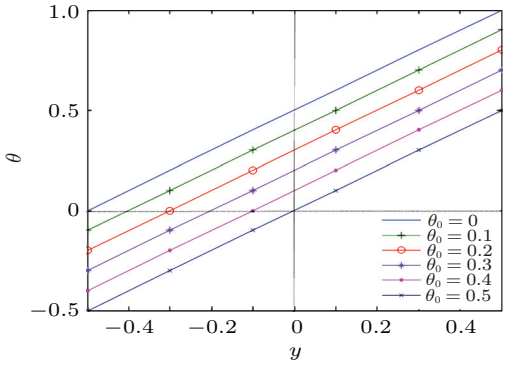

Fig. 2. Temperature profiles for variation in θ_0 spanning capped to open ends.

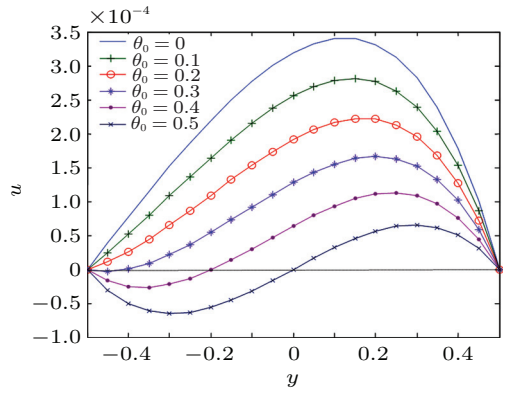

Fig. 3. Velocity profiles for $\alpha = 0.1$, $M = 3$ spanning capped to open ends.

Taking the limit $\alpha \to 0$ of the volume flow rate expression in Eq. (13) yields the result

$$Q \sim \frac{1}{M^2} \cdot \left(\frac{1}{2} - \theta_0\right)\left[1 - \frac{2}{M}\tanh\left(\frac{M}{2}\right)\right]\alpha^2 + O\left(\alpha^4\right). \tag{18}$$

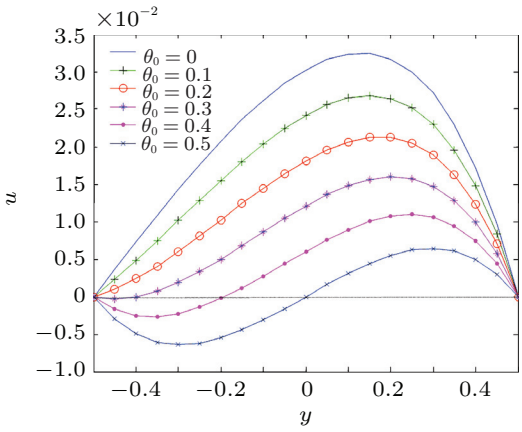

Fig. 4. Velocity profiles for $\alpha = 1.0$, $M = 3$ spanning capped to open ends.

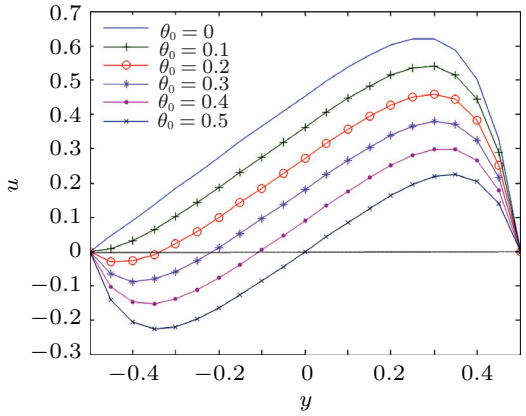

Fig. 5. Velocity profiles for $\alpha = 10$, $M = 3$ spanning capped to open ends.

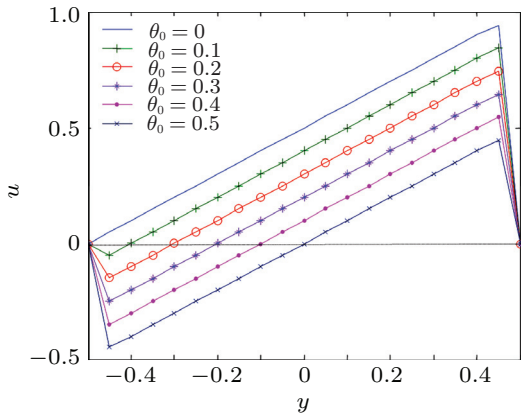

Fig. 6. Velocity profiles for $\alpha = 100$, $M = 3$ spanning capped to open ends.

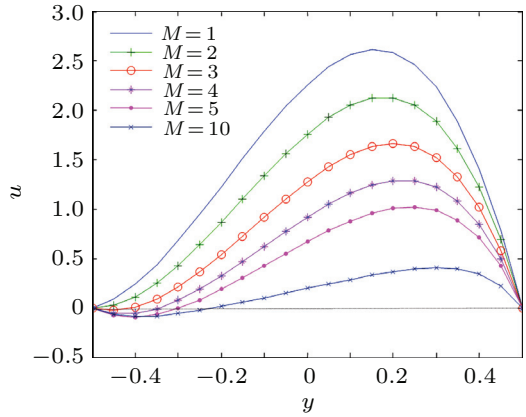

Fig. 7. Velocity profiles for $\alpha = 0.1$, $\theta_0 = 0.3$ spanning capped to open ends.

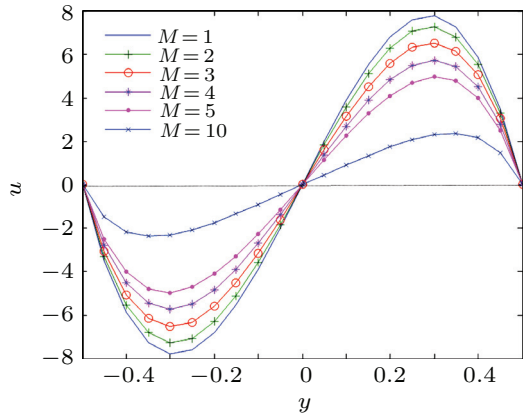

Fig. 8. Velocity profiles for $\alpha = 0.1$, $\theta_0 = 0.5$ spanning capped to open ends.

Finally, the limit $\alpha \to 0$ of condition (16) for incipient backflow gives the leading behaviour

$$(\theta_0)_c \sim \frac{1}{3} - \frac{\alpha^2 + M^2}{90} + O\left(\alpha^4\right). \tag{19}$$

The above leading behaviours are in agreement with the porous medium in the absence of magnetic field given in Ref. 1.

In the limit $\alpha \to \infty$ the leading behaviour of the velocity fluid is given in two parts, one for y positive and the other for y negative. The results are

$$u(y) \sim \begin{cases} y + \left(\frac{1}{2} - \theta_0\right) - \\ (1-\theta_0)\exp\left[\sqrt{\alpha^2+M^2}\left(y - \frac{1}{2}\right)\right], & y > 0, \\ y + \left(\frac{1}{2} - \theta_0\right) + \\ \theta_0 \exp\left[-\sqrt{\alpha^2+M^2}\left(y + \frac{1}{2}\right)\right], & y < 0. \end{cases} \tag{20}$$

Taking the $\alpha \to \infty$ limit of the volume flow rate in Eq. (13) yields

$$Q \sim \left(\frac{1}{2} - \theta_0\right)\left(1 - \frac{2}{\sqrt{\alpha^2 + M^2}}\right) + O\left(\alpha^3\right). \tag{21}$$

Finally, the $\alpha \to \infty$ limit of criterion (16) for incipient backflow is given by

$$(\theta_0)_c \sim \frac{1}{\sqrt{\alpha^2 + M^2}} + O\left(\alpha^3\right). \tag{22}$$

To study the effects of magnetic field and porous media on the flow field, the temperature and velocity profiles along with volume flux for various values of pertinent parameters are presented in Figs. 2–11. The influence of θ_0 on the dimensionless temperature profile is exhibited in Fig. 2. The velocity profile for six values of θ_0 is given in Figs. 3–6 for the respective values $\alpha = 0.1$, 1.0, 10 and 100 with the Hartmann number $M = 3$. It can be observed that an increase in θ_0 leads to a decrease in the velocity. The estimated feature to be observed is the tendency of the profiles toward straight lines as $\alpha \to \infty$ corresponds to pure Darcy flow which allows slip at the vertical wall. Indeed, as expected, the velocity and temperature profiles in the Darcy limit are identical.

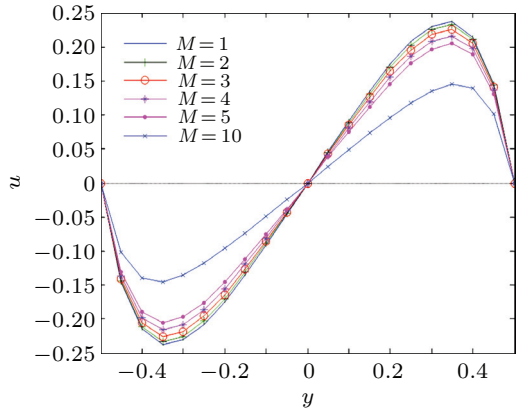

Fig. 9. Velocity profiles for $\alpha = 10$, $\theta_0 = 0.5$ spanning capped to open ends.

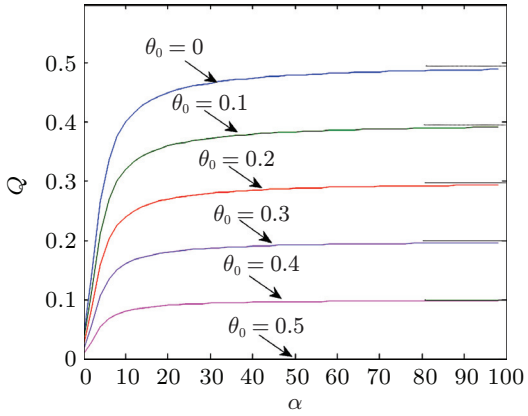

Fig. 10. Volume flux Q up the cavity for $M = 1$ as a function of α. The horizontal dotted lines give the asymptotic behaviour as $\alpha \to \infty$.

In accordance with the reported observations, the application of the transverse magnetic field will result in a resistive type force (Lorentz force) according to generalized Ohm's law, similar to drag force which tends to resist the fluid motion and thus reducing its velocity. Thus from the profiles in Figs. 7–9 we see that at any point of the channel, the velocity decreases with the increase in either M or θ_0.

Plots of the variation of volume flow rates may be analyzed from Figs. 10 and 11. An increase in θ_0 marks a significant reduction in the volume fluxes. The same is true for the Hartmann number M, and volume flux decreases as it increases. The asymptotic behaviour described by Eqs. (18) and (21) are presented in Figs. 10 and 11. The low α behaviour given by Eq. (19) and the high α behaviour described by Eq. (22) are compared with the numerically computed critical values $(\theta_0)_c$ as shown in Figs. 12 and 13. Moreover, from Figs. 12 and 13 the critical value of θ_0 for onset of back flow at the cold wall as a function of α can be observed. In Fig. 12 the values of $(\theta_0)_c$ for finite non-zero α and $\alpha \to 0$ (asymptotic behaviour) nearly coincide up to an extent in value of α ($\alpha = 0.1$ to $\alpha = 2$ approximately) whereas

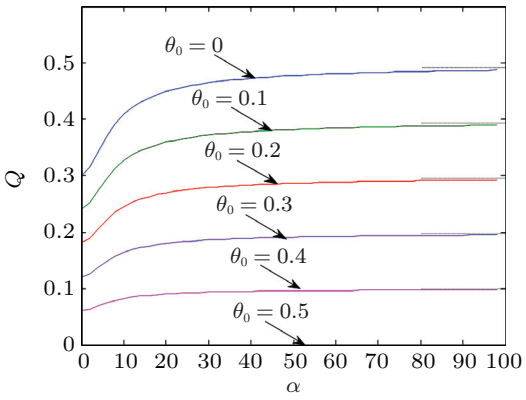

Fig. 11. Volume flux Q up the cavity for $M = 5$ as a function of α. The horizontal dotted lines give the asymptotic behaviour as $\alpha \to \infty$.

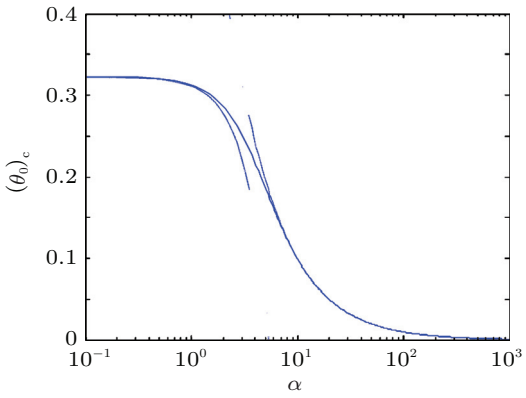

Fig. 12. Critical value of θ_0 for onset of backflow at the cold wall as a function of α for $M = 1$. The low and high α asymptotical behaviours for $\alpha \to 0$ and $\alpha \to \infty$ are shown as dotted lines, respectively.

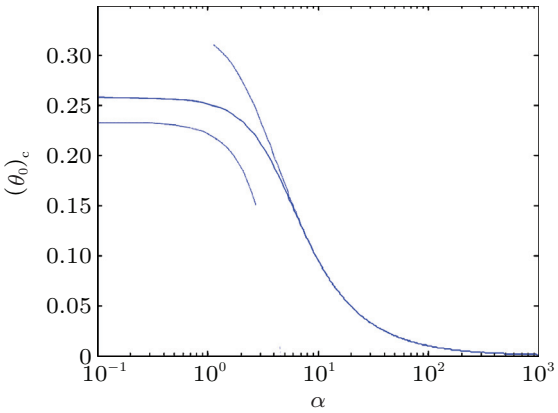

Fig. 13. Critical value of θ_0 for onset of backflow at the cold wall as a function of α for $M = 3$. The low and high α asymptotical behaviours for $\alpha \to 0$ and $\alpha \to \infty$ are shown as dotted lines, respectively.

in Fig. 13 we observe that the values of $(\theta_0)_c$ for finite non-zero α and $\alpha \to 0$ (asymptotic behaviour) differ right from the beginning. This difference in values observed is due to an increment in Hartmann number M. It is interesting to note that for finite non-zero α and $\alpha \to \infty$ (asymptotic behaviour), the profiles of $(\theta_0)_c$ are similar in nature to the increment of Hartmann number M.

1. P. D. Weidman, and A. Medina, Acta Mech. **199**, 209 (2008).
2. M. Turkyilmazoglu, Appl. Thermal. Eng. **35**, 127 (2012).
3. M. Turkyilmazoglu, Int. J. Thermal Sc. **51**, 195 (2012).
4. L. Prandtl, *Essentials of Fluid Dynamics* (Hafner Publishing Company, New York, 1952).
5. K. Bühler, Heat Mass Trans. **39**, 631 (2003).
6. P. D. Weidman, Heat Mass Transf. **43**, 103 (2006).
7. E. Magyari, Heat Mass Transf. **43**, 827 (2007).